Dynamic compression-shear loading with in-material interferometric measurements

H. D. Espinosa
School of Aeronautics and Astronautics, Purdue University, West Lafayette, Indiana 47907-1282

(Received 18 September 1995; accepted for publication 12 August 1996)

The present article introduces a new technique for window interferometry in the case of combined normal and shear wave motion. The method can, in principle, be used for micromechanical studies of damage and inelasticity in a variety of materials. Preliminary tests conducted on brittle materials indicate the feasibility of the technique and its advantages over other in-material measurements using embedded manganin gauges or electromagnetic particle velocity gauges. An analysis of the interferometric signals, incorporating variations in the index of refraction of the window material, is used in the interpretation of the velocity histories. The suitability of the technique in the study of dynamic failure and material instabilities is presented. Furthermore, the use of the in-material measurement technique in the design of pressure-shear recovery experiments is described. © *1996 American Institute of Physics.* [S0034-6748(96)00811-8]

I. INTRODUCTION

One of the major challenges in applied mechanics is the correlation between macroscopic events and processes occurring at the microlevel. The development of observation capabilities with spatial resolution of atomic dimensions, e.g., scanning tunneling microscopy (STM) and high resolution electron microscopy (HREM), has opened new frontiers in the mechanical characterization of advanced materials. Unfortunately, very limited effort has been directed towards the development of experimental techniques that would allow the identification and modeling of failure mechanisms from an atomic or molecular standpoint. Plate impact experiments offer unique features within the spirit of the stated needs. The experimental technique consists of generating normal and shear waves with a time resolution of a few nanoseconds and magnitudes up to several gigapascals (GPa), in specially designed target plates. In the case of recovery experiments, postshock examination of the specimens by means of STM, HREM, and other observational methodologies, allows the identification of failure mechanisms. These observations form the bases for (i) the comprehensive understanding of the processes occurring during shock deformation and (ii) the formulation of physically based constitutive models. Interferometric records, performed during the wave propagation event, are used as a diagnostic tool in the examination of derived or postulated models. The resolution and location, free surface or in-material, of these measurements are essential to the identification process. In this article, the in-material measurement techniques are investigated.

Several research efforts have been made for in material measurements of longitudinal and shear waves in dynamically loaded solids. The measurement of displacement or velocity histories at different depths within the material is especially valuable in its mechanical characterization. Damage, plasticity, phase transformations, and other material instabilities can be identified under stress conditions that are undisturbed by wave reflections from free surfaces. Gupta,[1] Young and Dubugnon,[2] and Gupta *et al.*,[3] reported successful experiments where velocity profiles have been obtained at interior surfaces by inserting metallic gauges in a magnetic field and measuring the current generated by their motion: these are called electromagnetic particle velocity (EMV) gauges. This technique can be applied only to nonmetallic materials. Furthermore, Feng and Gupta,[4] have shown that the thin epoxy bond, used in the assembly of EMV gauges, is responsible for the transmitted shear wave amplitude. Their computer simulations of pressure-shear experiments conducted in SiO_2 revealed that the visco-plastic response of the epoxy bond controls and limits the in-plane motion transmitted to the specimen. This phenomenon is highly undesirable in the study of damage and inelasticity in modern materials like ceramics and composites.

The other technique developed for in-material measurements, Williams and Keough,[5] Rosenberg and Bless,[6] employs manganin gauges placed between the specimen back face and a thick polymethyl methacrylate (PMMA) disk to measure the time history of the longitudinal stress σ_1. The measurement of the transverse stress, σ_2, is accomplished by placing another manganin gauge at an interface made in the direction of wave propagation. The shear stress is obtained as one half the difference between the two normal stresses, σ_1 and σ_2. A concern with this technique is the perturbation of the one dimensionality of the wave propagation due to the presence of a thin layer, perpendicular to the wave front, filled with a material having a different impedance and mechanical response. Calculations by Wong and Gupta,[7] show that the inelastic response of the material being studied affects the gauge calibration. Recently, Rosenberg and Brar,[8] reported that in the elastic range of the gauge material its resistance change is a function of the specimen elastic moduli. In a general sense, this is a disadvantage in the lateral stress gauge concept. Nonetheless, their analysis shows that in the plastic range of the lateral gauge response, a single calibration curve for all specimen materials exists. These findings provide a methodology for the appropriate interpretation of lateral gauge signals, and increase the reliability of the lateral stress measuring technique. Additional studies concerning the validity of the assumptions made in the work by Rosenberg and Brar,[8] and the role of

specimen inelasticity in gauge resistance change should be pursued.

The technique presented here is an extension, to the case of combined normal and shear motion, of the window interferometer introduced by Barker and Hollenbach.[9] It can be used for both of the techniques that produce pressure-shear loadings: oblique impact and normal impact with anisotropic crystals, such as Y-cut quartz, (Chhabildas and Swegle.)[10] The wave histories are obtained by direct measurement of displacements or particle velocities which are accomplished by manufacturing a high pitch diffraction grating at the specimen-window interface. A normal displacement interferometer (NDI), or a normal velocity interferometer [(NVI), Barker and Hollenbach],[11] and a transverse displacement interferometer [(TDI) Kim *et al.*][12] can be utilized.

This article starts with a description of pressure-shear with window interferometry, followed by a discussion of the experimental procedure used in the manufacturing of diffraction gratings within the window plate. The requirements on the window, in which the grating is embedded, are analyzed in detail. Experimental results obtained on a ceramic and a ceramic composite are presented together with some observations for future improvements in the interferometric in-material measurements. An analysis of the signals, incorporating variations in the index of refraction of the window material, is used in the interpretation of velocity histories. Applications of the technique to the study of dynamic failure and material instabilities are presented. Furthermore, the use of the in-material measurement technique in the design of a pressure-shear recovery experiment is described.

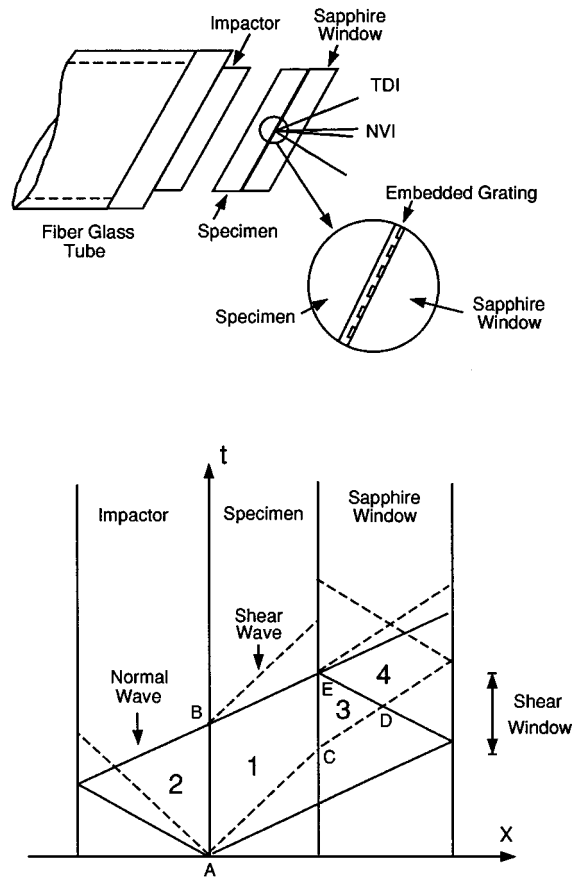

FIG. 1. Schematic of pressure-shear impact with window interferometry and corresponding t-X diagram.

II. PRESSURE-SHEAR EXPERIMENT WITH WINDOW INTERFEROMETRY

In this section, a plate impact experiment leading to combined dynamic loading is described. The experimental configuration is shown in Fig. 1(a). Compression-shear loading is accomplished by inclining the flyer and target plates with respect to the projectile axis. By varying the angle of inclination, a variety of loading states can be obtained. At impact, plane compression waves and shear waves are produced in both the impactor and the specimen. The elastic wave fronts for a plane wave analysis are given in a Lagrangian t-X diagram in Fig. 1. In the absence of a gap at the specimen-window interface, the major part of the compressive pulse propagates into the window, and the remainder, not shown in Fig. 1, is reflected due to a small mismatch in impedances. Another reflected pulse is generated when the transmitted compressive pulse reaches the free surface of the window. When this tensile pulse arrives at the specimen-window interface, slippage can take place due to the strong reduction in normal stress; therefore, useful information on the shear wave is limited to times less than the time corresponding to point E in Fig. 1. Similar features are encountered in the history of the shear wave.

One of the motivations for the development of the technique discussed here, is the elimination of states of pure shear stresses, or equivalently tensile and compressive stresses at 45°, that can develop within the specimen due to normal wave reflection at free surfaces. When the dynamic tensile strength of the material is a small fraction of the compressive strength, as is the case in ceramics and ceramic composites, failure of the material in tension prevents the identification of failure mechanisms under combined compression-shear loading. This failure mode was experimentally observed in WC/6Co anvil plates by Espinosa and Clifton.[13] Since pressure-shear impact experiments are especially suitable for the characterization of the dynamic shear resistance of materials under high strain rates and pressures, tensile failure is highly undesired in this type of experiment. The addition of a window plate to the target assembly moves the state of pure shear loading, region 4 in Fig. 1(b) to the window plate. The net effect is that this undesired stress state, within the specimen, is eliminated. It should be noted that the window material must withstand the pure shear loading state without damage and/or inelasticity.

The pressure-shear with window interferometry experiment presents several advantages over the other techniques mentioned previously. The method preserves the fundamental advantage that the measured wave profiles are undisturbed by reflections of the compressive wave at free surfaces. No interfaces are required that can perturb the one dimensionality of the wave propagation. The method can, in principle, be used for metallic and nonmetallic materials as long as a suitable window material, e.g., lithium fluoride, sapphire, glass, with a matching impedance can be found. The measurement of both longitudinal and shear waves are

made independently and at the same spatial point with a time resolution of approximately 2–3 nanoseconds. The independent measurement of normal and shear waves has the additional advantage that different interferometric techniques can be utilized on each measurement; for instance, TDI and NVI (see Fig. 2). Although a velocity interferometer can be used to monitor both waves simultaneously (Chhabildas *et al.*),[14] this approach has the major drawback that the sensitivity required by each wave component, normal and in-plane waves, is completely different, making the selection of the appropriate delay leg a difficult task. By contrast, the variable sensitivity of the TDI makes the experimental set up discussed in this article very suitable for the recording of low and high interface transverse velocities.

III. GENERAL EXPERIMENTAL PROCEDURE

Sapphire has been chosen as the window material because it remains transparent up to normal stresses of 15 GPa and it has an impedance that matches many ceramics and ceramic composites. Its spall strength is close to the Hugoniot elastic limit, which is of the order of 20 GPa in the Z direction. This stress is considerably larger than the stresses encountered in the experiments reported here, therefore, the window material remained elastic. Therefore, difficulties in the interpretation of the experimental records associated with inelasticity in the window material, are not expected.

For the experiment to be successful, the specimen-window interface should transmit the in-plane motion without damage or plastic flow. In addition, a grating that can generate the necessary diffracted beams for the measurement of transverse velocities is required. The manufacturing of a multilayer tailored interface, described next, meets both of these requirements. Moreover, considering that the film can be made a few microns thick, a negligible perturbation to the longitudinal and/or shear waves, due to impedances mismatch, is expected.

A Ronchi ruling grating made of Ti strips is embedded within the sapphire window. The process starts with the sputtering of a Ti layer 100 nm thick. Then, by using standard photolithographic techniques a photoresist mask 1 μm thick is constructed with the desired pitch. The exposed Ti is chemically etched by using an etchant with the composition: distilled water 100 ml hydrofluoric acid (40%) 1 ml, and nitric acid 2 ml (Kroll's reagent). Alternatively, reactive ion etching (RIE) using CF_4+8% O_2 successfully etched Ti with the following parameters: rf power per unit area=0.4 W/cm^2, bias voltage=560 V, total chamber pressure=20 mT, CF_4 flow rate=37 sccm, O_2 flow rate=3 sccm, and Dwell time =1.2 s. RIE was needed in the manufacturing of submicron gratings; up to 600 l/mm gratings have been made with this procedure.

After removing any remnant photoresist, an Al_2O_3 layer with thickness between 5–10 μm, is sputtered onto the sapphire substrate containing the diffraction grating. Al_2O_3 amorphous thin films of high quality, characterized by their transparency, adhesion to the substrate, layer uniformity and good stoichiometry, have been obtained. The parameters used were, rf power=5 W/cm^2, chamber pressure=30 mT, and a distance between the Al_2O_3 target (99.99% purity) and the sapphire substrate of 1.4 in. The rate of deposition was 20 nm/min. In order to avoid cracking due to the generation of thermal stresses in the substrate and target, both target plate and the window plate were maintained at room temperature by a cooling capability incorporated in the design of the sputtering machine.

The selection of the Ti thin film as the reflecting part of the grating is based on its strong adhesion to sapphire. Peel tests conducted by Kim *Y et al.*[15] show that Ti deforms plastically when it is bonded to sapphire substrates. This behavior was rationalized by the elastic properties of the substrate and the chemical reaction at the interface where the oxygen present in the sapphire microstructure contributes to the formation of a TiO_2 transition film. An important feature of the multilayer embedded grating is that the Ti strips are confined by the surrounding Al_2O_3 film. Hence, the shear resistance of the layer is mainly controlled by the alumina thin film quality (porosity, atomic structure).

The frictional properties of the specimen-window interface are utilized to transmit the in-plane motion. To do this, the Al_2O_3 thin film on the sapphire window, is lapped to a flatness better than 2 Newton rings (under monochromatic light λ=587.6 nm) and its roughness increased by using 15 μm diamond paste. It should be noted that the frictional requirements at the specimen-window interface are less stringent than at the impact surfaces, because the pressure wave arrives at the interface before the shear wave [see Fig. 1(b)].

The specimen and window plates are assembled in a clean room. After they are clamped together, small epoxy drops are applied at the edges. Neither epoxy nor alumina-filled epoxy are used at the specimen-sapphire window interface because they strongly limit the level of shear tractions that can be transmitted to the window material (see Feng and Gupta).[4]

IV. ANALYSIS OF NVI AND NDI FOR WINDOW INTERFEROMETRY

When a window material is used, the light rays reflected from the specimen-window interface must pass through a window region in which the wave motion has produced variations in the index of refraction. These variations alter the Doppler-frequency shift of the reflected laser light; therefore, new expressions for the calculation of displacements (Michelson interferometer) and velocities (Velocity interferometer) must be derived.

Following Clifton,[16] consider two rays which arrive at the photodetector simultaneously (see Fig. 3). Their relative phases can be determined by tracing these rays backward until a fixed position in the incident laser beam is reached.

If $\hat{t}$ denotes the times at which the two light rays arrive at the photodetector, then the time at which these rays leave the reference plane are (see Fig. 3):

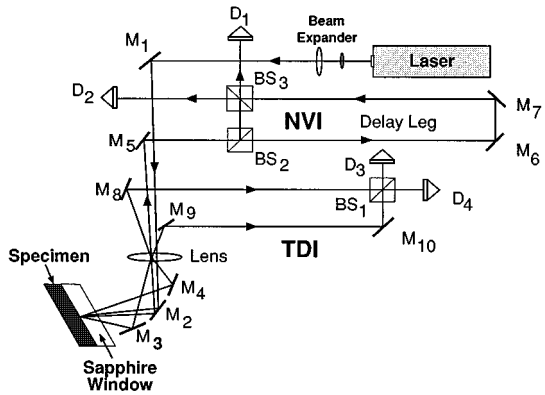

FIG. 2. Optical layout of combined NVI-TDI interferometers.

$$t_2=\hat{t}-\frac{A}{c_0}-\frac{2L}{c_0}-2(H-c_1t)\frac{n_0}{c_0}-\frac{2}{c_0}\int_{U(t)}^{c_1t}ndx$$

$$t_1=\hat{t}-\tau-\frac{A}{c_0}-\frac{2L}{c_0}-2[H-c_1(t-\tau)]\frac{n_0}{c_0}-\frac{2}{c_0}\int_{U(t-\tau)}^{c_1(t-\tau)}ndx, \tag{1}$$

where τ is the delay time, H is the window thickness, A and L arbitrary lengths used in the interferometer set up, n_0 is the refractive index of the unstressed window material, n is the refractive index of the stress window material, $U(t)$ is the specimen-window interface normal displacement, c_0 is the speed of the laser light, and c_1 is the longitudinal shock wave speed. In the NVI shown in Fig. 2, the reference plane can be identified with the location of mirror M5, A with the ray path length from M5 to BS3, and L with the ray path length from M5 to the window back surface.

The time difference of the two rays leaving the reference plane is

$$t_2-t_1=\tau+2c_1\tau\frac{n_0}{c_0}-\frac{2}{c_0}\left\{\int_{U(t)}^{c_1t}ndx-\int_{U(t-\tau)}^{c_1(t-\tau)}ndx\right\}. \tag{2}$$

The refractive index n may be related to the normal stress in the window by an expression of the form $n=n_0-\alpha\sigma$; $\alpha>0$ where α is a constant. Substitution of this expression into the integrals gives,

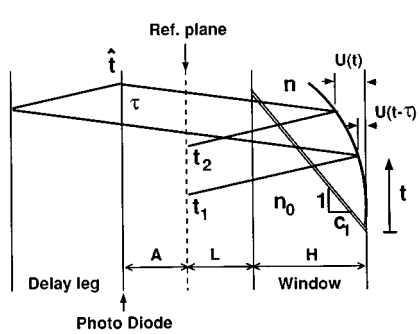

FIG. 3. Lines of constant phase along direct and indirect light ray paths.

$$t_2-t_1=\tau+2c_1\tau\frac{n_0}{c_0}-\frac{2}{c_0}\left\{\int_{U(t)}^{c_1t}(-\alpha\sigma)dx+\int_{U(t-\tau)}^{c_1(t-\tau)}(\alpha\sigma)dx+n_0[c_1t-U(t)-c_1(t-\tau)+U(t-\tau)]\right\}. \tag{3}$$

Furthermore, the integrals in space can be converted to integrals, over time, of the velocity at the specimen-window interface by using characteristic equations within the window. Substituting the integrand, σdx, by $(-\rho c_1\dot{U})c_1dt$, the time difference between the light rays becomes

$$t_2-t_1=\tau+2c_1\tau\frac{n_0}{c_0}-\frac{2}{c_0}\left\{\int_0^{t}(\alpha\rho c_1^2\dot{U})dt-\int_0^{(t-\tau)}(\alpha\rho c_1^2\dot{U})dt+n_0[c_1t-U(t)-c_1(t-\tau)+U(t-\tau)]\right\}. \tag{4}$$

Then,

$$t_2-t_1=\tau+\frac{2}{c_0}(n_0-\alpha\rho c_1^2)[U(t)-U(t-\tau)]. \tag{5}$$

The change in phase, expressed in numbers of fringes from the onset of motion of the interface is given by

$$F\equiv\frac{\omega[t_2-t_1-\tau]}{2\pi}=\frac{2\omega}{2\pi c_0}(n_0-\alpha\rho c_1^2)[U(t)-U(t-\tau)], \tag{6}$$

in which ω is the frequency of the laser source. Since $\omega=2\pi c_0/\lambda$, the fringe count can be expressed in terms of the laser wave length λ, namely,

$$F=\frac{2}{\lambda}(n_0-\alpha\rho c_1^2)[U(t)-U(t-\tau)]. \tag{7}$$

If the interface moves smoothly so that $U(t)-U(t-\tau)=u(t-\tau/2)\tau+O(\tau^2)$, then the interface normal velocity u at time $t-\tau/2$ is given by

$$u\left(t-\frac{\tau}{2}\right)\simeq\frac{\lambda F}{2\tau(n_0-\alpha\rho c_1^2)}. \tag{8}$$

A similar analysis can be carried out for the case in which the normal shock wave has been reflected from the window free surface, i.e., $t>H/c_1+\tau$. In this case, the expression for F is

$$F=\frac{2\tau}{\lambda}\{(n_0-\alpha\rho c_1^2)u(t-\tau/2)-(n_0-1)u_{fs}(t-\tau/2)+2\alpha\rho c_1^2u[2(t-H/c_1)-\tau]\}. \tag{9}$$

Assuming the window material remains elastic, we have that the window free surface velocity is equal to two times the interface velocity at time $t-H/c_1$, i.e., $u_{fs}(t)=2u(t-H/c_1)$, then the fringe count can be made a function

only of the particle velocity at the specimen-window interface. For sapphire $n_0-\alpha\rho c_1^2 \simeq 1.777$, $(1-n_0)\simeq -0.78$ and $\alpha\rho c_1^2 \simeq 0$. Hence,

$$F \simeq \frac{2\tau}{\lambda}\{1.777u(t-\tau/2)-1.56u(t-H/c_1-\tau/2)\},$$

$$\text{for } t>H/c_1+\tau$$

$$F \simeq \frac{2\tau}{\lambda}\{1.777u(t-\tau/2)\} \quad \text{for } \tau<t<H/c_1. \tag{10}$$

If the analysis were repeated for a displacement interferometer, the analysis would be the same as for $\tau\rightarrow\infty$. Then, for NDI:

$$F=\frac{2}{\lambda}(n_0-\alpha\rho c_1^2)U(t)+\frac{4}{\lambda}(1-n_0)U(t-H/c_1)$$

$$+\frac{2}{\lambda}\alpha\rho c_1^2 U[2(t-H/c_1)]. \tag{11}$$

For sapphire we have:

$$F \simeq \frac{2}{\lambda}\{1.777U(t)-1.56U(t-H/c_1)\}. \tag{12}$$

The frequency $\dot{F}$ is related to the interface normal velocity according to

$$f \equiv \dot{F}=\frac{2}{\lambda}\{1.777u(t)-1.56u(t-H/c_1)\}. \tag{13}$$

The expressions derived in this section will be used in the calculation of the interface velocity histories measured in the pressure-shear experiments discussed in the next section.

In closing this section, it should be noted that variations in the window index of refraction equally and simultaneously alter the Doppler-frequency shift of the two n^{th} order diffracted beams used in the transverse displacement interferometer (TDI). Therefore, the expression for the time varying phase function

$$\Psi(t)=\frac{4\pi}{\lambda}\left[V\left(t-\frac{l}{c}\right)\sin\theta_n\right], \tag{14}$$

derived by Kim *et al.*,[12] remains unchanged. A different scenario appears in the case of the variable sensitivity displacement interferometer (VSDI) developed by Espinosa *et al.*[17] In this case, the corrections presented in this section must be incorporated in the expression for the time varying phase function because the nth order diffracted beam and 0th order beam used in the VSDI have different path lengths within the window.

V. EXPERIMENTAL RESULTS

Pressure-shear with window interferometry experiments were performed in a 2.5-in light gas gun at Brown University. Sapphire windows 1 in. in diameter, 3.2-mm-thick were used. A grating with an area of 7 mm×4 mm and 200 lines/mm was manufactured in the middle of the windows following the procedure described in Sec. III. Additional details of the experiments are given in Table I. The compression and shear wave behavior were recorded by monitoring the time resolved motions of the specimen-sapphire interface with normal velocity and transverse displacement interferometric techniques (NVI and TDI), Figs. 1 and 2. The measurements were recorded on a transient digital oscilloscope with a sampling period of 0.742 ns per data point. The interference fringes measured with the TDI were first filtered by using a Fast–Fourier transform method. The filtered amplitudes of the fringes were then scaled to obtain uniform fringe amplitude. By numerical differentiation, the transverse velocity versus time profile was obtained. Details of the data reduction process can be found in Tong W.[18] Similar data processing was used for the NVI, except that differentiation was not required. As discussed in the previous section, the relationship between the number of fringes and the particle velocity being measured must account for the refractive index changes of the window. Before the longitudinal wave reaches the free surface of the window, this relationship is given by Eq. (8). Since the form of this equation can be related to the form given by Baker and Hollenbach,[11] the frequency corrections obtained by them for sapphire, when the wave propagates along the Z-axis of the crystal, are used in the interpretation of the experimental records reported here.

TABLE I. Summary of experimental results.

Shot No.	Projectile velocity	Skew angle	Specimen material/thickness	Impactor material
-	V_0, [mm/μs]	α, [deg]	h, [mm]	
91-04	0.231	18	AlN/AlN/Al/4.028	AlN/AlN/Al
91-07	0.124	22	Vistal/4.020	WC/6Co
95-09	0.158	18	GRP/0.370	Steel

Time resolved velocity profiles for a compression-shear experiment performed on an AlN/AlN/Al ceramic composite, developed by Lanxide Armor Products, Inc., are displayed in Figs. 4 and 5. The composite consists of aluminum nitride (AlN) reinforcement particles with a mean diameter of 3 μm and a matrix of AlN/Al. The compressive wave

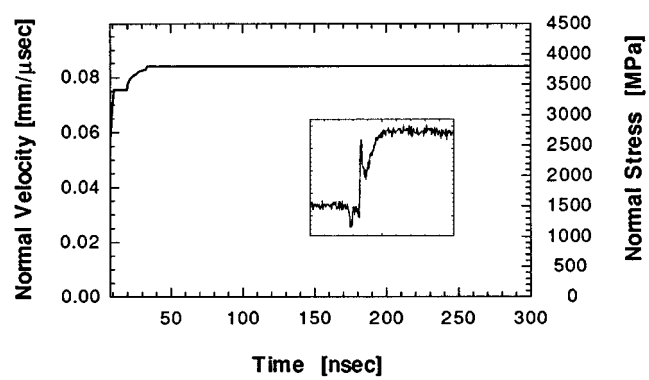

FIG. 4. Normal particle velocity as a function of time measured at the AlN/AlN/Al specimen-sapphire interface, Shot 91-04. The inside box reproduces the laser interferometer trace as recorded by the oscilloscope.

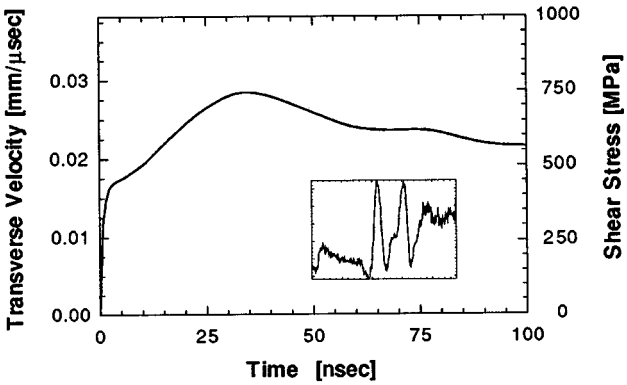

FIG. 5. Transverse particle velocity-time measured at the AlN/AlN/Al specimen-sapphire interface, Shot 91-04. The inside box reproduces the laser interferometer trace as recorded by the oscilloscope.

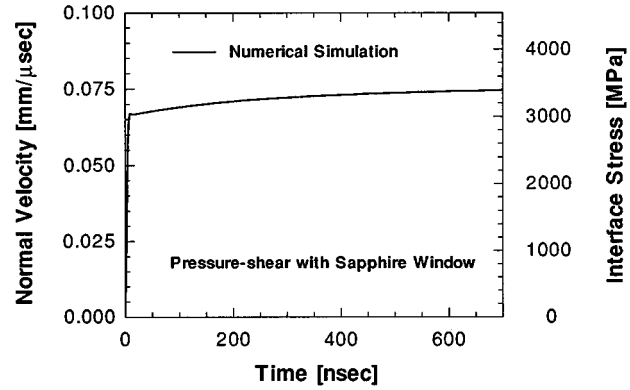

FIG. 7. Normal velocity-time profile predicted by the model proposed by Espinosa *et al.* (Ref. 19) for Alumina, Shot 91-07.

shows a jump in particle velocity followed by a ramp-wave structure. This profile is consistent with an initial elastic limit followed by a dynamic hardening region; however, the ramp may also be associated with closure of rough surfaces at the specimen-window interface. The shear wave shows a similar structure in the first 30 ns. The amplitude corresponding to an elastic response is attained. The peak shear stress is $\tau=750$ MPa. The decreasing shear stress observed at later times can be attributed to wave attenuation due to inelastic strain rates developing behind the wave front. Nonetheless, the proper interpretation of this feature requires further characterization of the shear resistance of the Al_2O_3 thin film and the frictional properties of the specimen-window interface.

The same experimental configuration, Shot 91-07, has been used successfully for conducting a test addressing the dynamic shear resistance of an alumina manufactured by Coors Co. under the trade name Vistal (99.99% alumina). The trace from the normal displacement interferometer is shown in Fig. 6. During the first 275 ns, the frequency of the input signal exceeded the frequency response of the digital oscilloscope. Upon arrival of the longitudinal wave to the window free surface, the frequency was low enough for its recording. The observed low frequency signal is the result of the frequency becoming a function not only of the specimen-window interface normal velocity but also a function of the window free surface velocity. The expression for this frequency was derived in Sec. IV, Eq. (13), and it can be written in terms of the free surface velocity, u_{fs}, by using the relation $u_{fs}(t)=2u(t-H/c_1)$. Hence,

$$f(t)=\frac{2}{\lambda}[1.77u(t)-0.78u_{fs}(t)]. \tag{15}$$

Based on this expression for the frequency at time t, interpretation of the experimental records can be accomplished by performing a numerical simulation of the pressure-shear experiment with the model derived by Espinosa *et al.*[19] for ceramics containing a glassy phase between alumina grains. Comparison of the measured signal frequency and the frequency obtained from Eq. (15), when the numerically computed velocity histories u_{fs} and u are used, provides a means for further identification of the material response. The computed velocity-time profile is given in Fig. 7. The parameters used in the model are those reported in the article by Espinosa *et al.*,[19] except for the value of $\overline{\sigma^*}$ which is taken equal to 850 MPa. This higher value of $\overline{\sigma^*}$ is justified if one takes into account the strong pressure-sensitivity of the glass flow stress.[19,20] The velocity profile shows a monotonically increasing stress in agreement with the features present in the velocity-time profiles reported by Munson and Lawrence[21] in their study of pure alumina. The experimental and numerically computed frequencies are plotted in Fig. 8. The good agreement in the initial value and the slope of the curve suggests that the model prediction of the normal particle velocity is quite accurate. The measured transverse particle velocity at the specimen-window interface

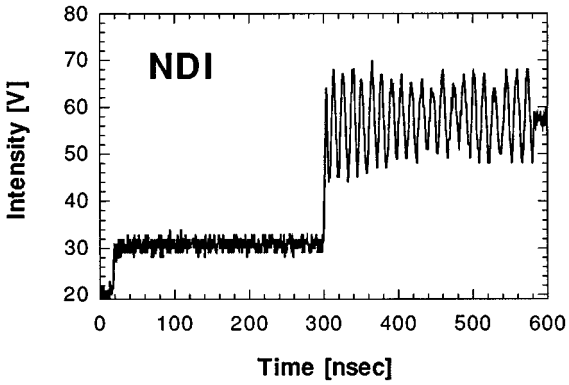

FIG. 6. Normal displacement interferometer trace for pressure-shear experiment with window interferometry performed on alumina, Shot 91-07.

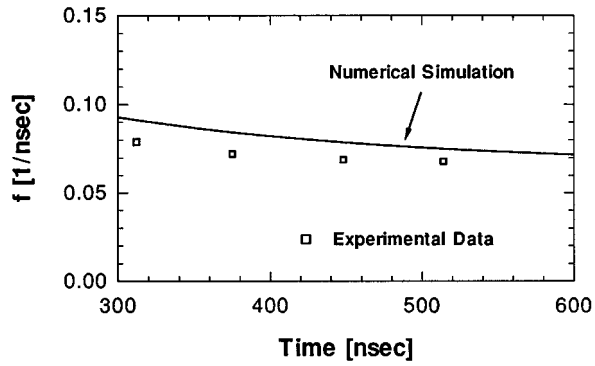

FIG. 8. Comparison between experimental and numerical frequence after the arrival of the compressive wave to the window free surface, Shot 91-07.

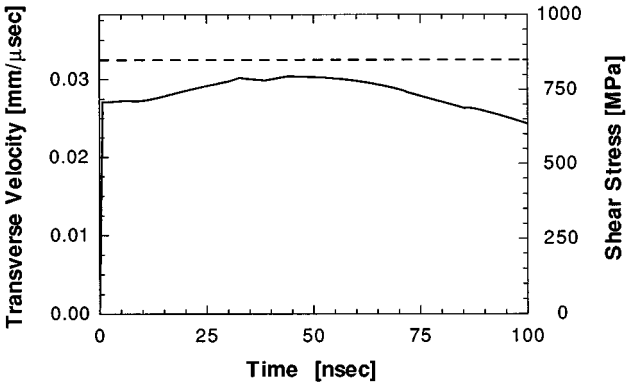

FIG. 9. Experimental transverse particle velocity-time profile for Alumina, Shot 91-07.

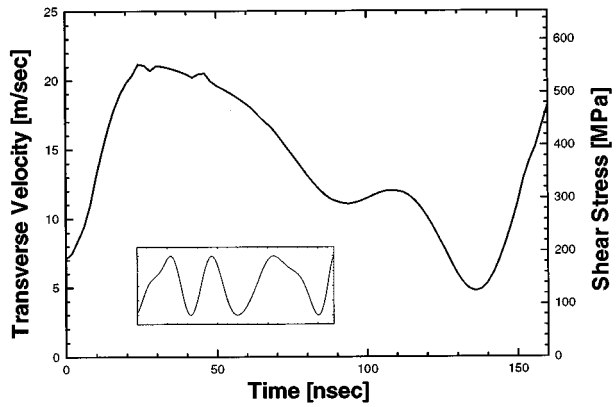

FIG. 10. Transverse particle velocity-time measured at the glass reinforced polyester specimen-sapphire interface, Shot 95-09. The inside box reproduces the TDI trace after amplitude correction.

is shown in Fig. 9. This velocity is essentially constant with magnitude very close to the elastic prediction, dash line in Fig. 9. Therefore, even if energy dissipation takes place during the normal wave propagation event, the shear resistance of high purity alumina (99.99% alumina) remains almost unchanged at these stress levels.

Recently, a pressure-shear impact experiment conducted at Purdue University, in a 3-in light gas gun, provided additional insight about the feasibility and resolution of in-material interferometric measurements. In this experiment, Shot 95-09, the impactor consisted in a 370-μm-thick glass reinforced polyester woven composite (GRP) backed by a speed star steel (AISI type $M2$ tool steel) plate 5.74-mm-thick. A sapphire window, 1.5 in. in diameter and 6-mm-thick, was used as target plate. A 600 lines/mm grating was embedded in the window by means of the procedure described in Sec. III. A TDI was employed to measure in-plane motion and a differential normal displacement interferometer (DNDI) was used to record normal motion. The DNDI was obtained by combining the 0th order beam reflected from the embedded grating and the reflected beam from the back surface of the sapphire window. The displacement-fringe count relation for the DNDI can be derived from the formulas discussed in Sec. IV, namely,

$$U(t)=\frac{\lambda}{2(n_0-\alpha\rho c_1^2)}F(t) \quad \text{for } t<\frac{H}{c_1}$$

$$U(t)=\frac{\lambda}{2(n_0-\alpha\rho c_1^2}F(t)+2U(t-H/c_1)$$

$$\text{for } t>\frac{H}{c_1}. \tag{16}$$

In the above expression, the free surface displacement at time t was expressed in terms of the interface displacement at time $t-H/c_1$.

The transverse velocity profile and corresponding amplitude corrected signal are given in Fig. 10. We can observe that the transverse velocity increases to a maximum of 21 m/s and then progressively decreases. This reduction in in-plane velocity can be the result of several processes; inelastic behavior of the composite sample, interface sliding, and/or inelasticity of the coating used to embed the grating in the window plate. The last mechanism appears to be the most likely in view that alumina coatings, manufactured by sputtering, are in general amorphous. It is known that amorphous materials develop shear instabilities at room temperature which can result in the observed reduction in transverse velocity, Steif *et al.*[22] More experiments are required to understand the mechanism leading to this observation. After about 200 ns, the TDI fringe contrast was reduced significantly making its interpretation difficult. The reduction in fringe contrast in the TDI can be indicative of grating modification due to plastic flow of the Ti strips. One avenue for improvement is to embed the reflective strips within the sapphire substrate, by appropriate reactive ion etching of the sapphire window, eliminating the need of the Al_2O_3 thin coating. Alternatively, manufacturing of a coating with a high shear strength is required.

The normal velocity history recorded by the differential displacement interferometer previously discussed is shown in Fig. 11. The amplitude corrected signal is included in the same figure. Since sapphire and steel have similar longitudinal impedances, the trace presents a velocity history typical of the pressure-shear sandwich configuration, Espinosa and Clifton.[13] The normal stress increases as a function of the number of waves reverberations within the specimen. It should be noted that a homogeneous state is not achieved before the arrival of the release wave generated at the free surface of the window plate. Two factors appear to contribute to this behavior. The existence of a small gap between the composite sample and the backing steel plate, and the composite inelastic behavior. The effect of the gap can be observed as a reduction in normal velocity at approximately 150 ns. Concerning the composite high strain rate response, we expect significant inelastic deformations due to the woven microstructure and the soft polyester matrix.

VI. DISCUSSION AND APPLICATIONS TO RELATED RESEARCH

The methodology presented here opens several possibilities for fundamental studies of micromechanics of inelastic deformation and damage in solids. The technique allows the measurement of transverse particle velocities at a range of distances from the impact surface, including positions that

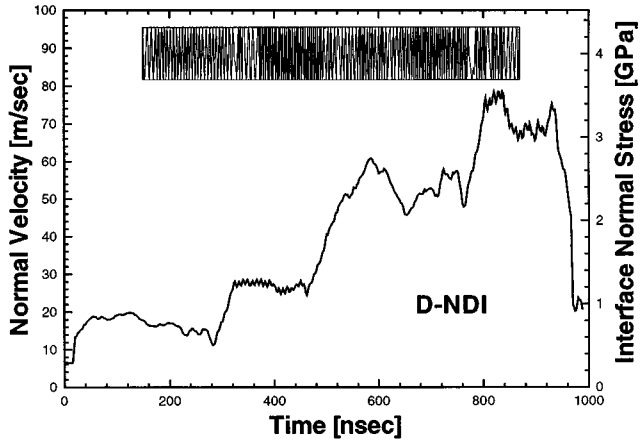

FIG. 11. Normal particle velocity-time measured at the glass reinforced polyester specimen-sapphire interface, Shot 95-09. The inside box reproduces the D-NDI trace after amplitude correction.

are very close to the impact surface. By placing the point of observation at different depths within the material, direct determination of shear stress-time histories can be obtained. This feature is of great interest for clarification of the reported strong reduction in shear strength together with the development of failure waves in glasses, Brar *et al.*,[23] Kanel.[24] The approach should also be valuable in understanding the complex wave structure that arises in solids undergoing phase transformations and shear localization.

An important application of window interferometry is encountered in the design of a pressure-shear recovery experiments.[17,20] Details of the configuration are given in Figs. 12 and 13. In this configuration, the momentum trap plate is made of a window material to allow the measurement of normal and in-plane motions at the back surface of the sample. The simultaneous trapping of the longitudinal and shear momentum, by the window plate, is accomplished by manufacturing a multilayer flyer plate (see Figs. 12 and 13). Such a flyer consists of a polymer thin film, approximately 1 μm thick sandwiched between two thicker hard plates, see Espinosa *et al.*[17] for more details. A similar design has been proposed by Yadav *et al.*,[25] but a lubricant was used instead. The use of a very thin film is essential to the minimization of the time required for the achievement, within the thin film, of the normal stress imposed at the impact surface. Due to impedance mismatch between the thin film and the bounding plates, several wave reverberations are needed for the attainment of the maximum normal stress. We have shown, Espinosa *et al.*,[17] that the normal wave unloading produced by the polymer thin film does not

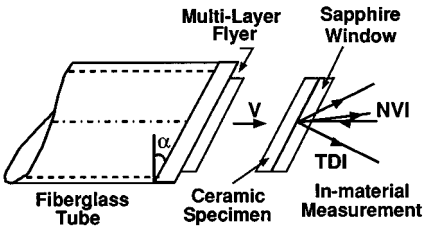

FIG. 12. Pressure-shear soft-recovery configuration.

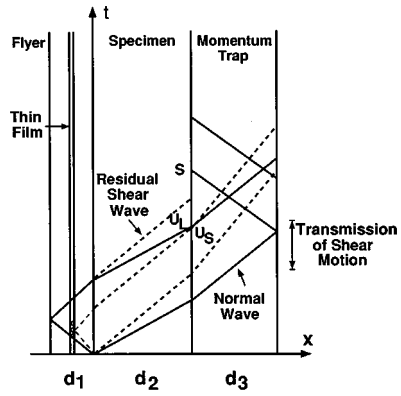

FIG. 13. Lagrangian *t-X* diagram for *pressure-shear recovery* experiment with multiplate flyer and window-momentum trap plate.

result in significant shear stress reduction and/or interfacial sliding at the impact surface. We have also observed that film uniformity minimizes the tilt between the flyer plates which can perturb the interferometric measurement of the in-plane motion. The resulting elastic wave fronts are shown in Fig. 13. The indicated residual shear wave is the result of the small but finite shear resistance of the thin film material and the inability of the specimen-momentum trap interface to transfer shear motion upon the unloading of the longitudinal wave.

We have shown that in-material measurement of combined transverse and normal motions with interferometric techniques is feasible. A NDI, or a NVI, and a TDI were successfully utilized. The wave histories were obtained by embedding a high pitch diffraction grating at the specimen-window interface. Longitudinal and shear waves measurements, at the same spatial point with a time resolution of 2–3 ns, were made in ceramic and composite samples. The better spatial and time resolution of this technique, when compared to manganin and electromagnetic gauges, make the window interferometer a valuable tool for the measurement of normal and shear wave speeds as well as the study of damage and inelasticity of modern materials. It should be noted that manufacturing of the grating within the window material, to eliminate the need of a thin amorphous film that can control the transmitted shear wave amplitude, may be needed. Since the technique does not require special modifications of the plate impact facilities, it can be easily applied in most shock-wave laboratories.

ACKNOWLEDGMENTS

This research was supported by the National Science Foundation through Grant Nos. MSS-9309006 and MSS 9311289. The author wishes to thank R. J. Clifton for his insightful suggestions and comments during this work, and D. Dandekar for facilitating blue prints and other materials during the development of the impact facility employed in the experimental work reported here.

[1] Y. M. Gupta, Appl. Phys. Lett. **29**, 694 (1976).
[2] Z. Young and O. Dubugnon, Int. J. Rock Mech. Min. Sci. **14**, 247 (1977).
[3] Y. M. Gupta, D. D. Keough, D. F. Walter, K. C. Dao, D. Henley, and A. Urweider, Rev. Sci. Instrum. **51**, 183 (1980).

[4] R. Feng and Y. M. Gupta, in *AIRAPT/APS Meeting, Topical Group on Shock Compression of Condensed Matter*, edited by S. C. Schmidt (Elsevier, New York, 1993).
[5] R. Williams and D. D. Keough, Bull. Am. Phys. Soc. **12**, 1127 (1968).
[6] Z. Rosenberg and S. J. Bless, Experimental Mechanics, **26**, 279 (1986).
[7] M. K. W. Wong, and Y. M. Gupta, in *Shock Compression of Condensed Matter*, edited by S. C. Schmidt, R. D. Dick, J. W. Forbes, and D. J. Tasker (Elsevier, Essex, U.K., 1991).
[8] Z. Rosenberg and N. S. Brar, in *AIRAPT/APS Meeting, Topical Group on Shock Compression of Condensed Matter*, edited by S. C. Schmidt (Elsevier, New York, 1993).
[9] L. M. Barker and R. E. Hollenbach, Rev. Sci. Instrum. **36**, 1617 (1965).
[10] L. C. Chhabildas and J. W. Swegle, J. Appl. Phys. **51**, 4799 (1980).
[11] L. M. Barker and R. E. Hollenbach, J. Appl. Phys. **41**, 4208 (1970).
[12] K. S. Kim, R. J. Clifton, and P. Kumar, J. Appl. Phys. **48**, 4132 (1977).
[13] H. D. Espinosa and R. J. Clifton, in Symposium on Experiments in Micromechanics of Fracture-Resistant Materials (ASME Winter Annual Meeting), edited by K. S. Kim, Atlanta, Georgia, 1991(unpublished), pp. 37–56.
[14] L. C. Chhabildas, H. J. Sutherland, and J. R. Asay, J. Appl. Phys. **50**, 5196 (1979).
[15] Y. H. Kim, Y. S. Chang, N. J. Chou, and J. Kim, J. Vac. Sci. Technol. A **5**, 2890 (1987).
[16] R. J. Clifton, J. Appl. Phys. **41**, 5335 (1970).
[17] H. D. Espinosa, M. Mello, and Y. Xu, J. Appl. Mech. (in press).
[18] W. Tong, Ph.D. thesis, Brown University, Providence, RI (1991).
[19] H. D. Espinosa, G. Raiser, R. J. Clifton, and M. Ortiz, J. Hard Mater. **3**, 285 (1992).
[20] H. D. Espinosa, Ph.D. thesis, Brown University, Providence, RI (1992).
[21] D. E. Munson and R. J. Lawrence, J. Appl. Phys. **50**, 6272 (1979).
[22] P. S. Steif, F. Spaepen, and J. W. Hutchinson, Acta Metall. **30**, 447 (1982).
[23] N. S. Brar, Z. Rosenberg, and S. J. Bless, J. Phys. C **1**, 639 (1991).
[24] G. I. Kanel, S. V. Rasorenov, and V. E. Fortov, in *Shock Compression of Condensed Matter*, edited by S. C. Schmidt, R. D. Dick, J. W. Forbes, and D. J. Tasker (Elsevier, Essex, U.K., 1991).
[25] S. Yadav, J. A. Davis, and K. T. Ramesh, in Experimental Techniques in the Dynamics of Deformable Solids, ASME AMD, 1993 (unpublished), Vol. 165, pp. 71–78.